SENSING CHARACTERISTICS OF PLASMONICS INTEGRATED IN VARIOUS CONFIGURATIONS OF PLASTIC OPTICAL FIBER PROBE

FARAH WARDINA BINTI S FENDI

UNIVERSITI SAINS MALAYSIA

2025

SENSING CHARACTERISTICS OF PLASMONICS INTEGRATED IN VARIOUS CONFIGURATIONS OF PLASTIC OPTICAL FIBER PROBE

by

FARAH WARDINA BINTI S FENDI

**Thesis submitted in fulfilment of the requirements
for the degree of
Master of Science**

August 2025

ACKNOWLEDGEMENT

I want to thank Allah SWT for the opportunity to complete my study. Completing this thesis is not an easy journey. However, I made it through with endless support from countless individuals.

Firstly. I would like to express my gratitude to my supervisor, Assoc. Prof. Dr. Mundzir bin Abdullah, for his insightful guidance and endless support in completing this work. His contributions made this process both challenging and rewarding. Thanks to my co-supervisors, Dr. Wan Maisarah and Dr. Ahmad Shazwan, for helping me with their opinions and knowledge.

To my family, Ayah, Mama, Abang, Ebi, and Adik, your love and unwavering support gave me the strength to carry on and finish this study. I acknowledge all of your sacrifices and support and am profoundly grateful for them.

To my friends, thank you for your help and understanding. Without you guys, this journey would be extra lonely and more stressful. I want to thank Nasuha, Azira, Atikah, Syahida, Faridah, Imdad, Ainita, Anis, Aizat, and Saleh for their support. Moreover, I also want to express my gratitude to the people of INOR, USM, and MARA who have helped me since the first day I started my studies.

Finally, thank you to myself for working hard and never giving up when life is treating you hard. Thank you for always learning from mistakes and growing up to be the person we always want to be when we become adult. Let's continue to be the example of kindness and resilience, even when the situation is unfair, difficult, and seems endless.

TABLE OF CONTENTS

ACKNOWLEDGEMENT ii

TABLE OF CONTENTS iii

LIST OF TABLES vii

LIST OF FIGURES viii

LIST OF SYMBOLS x

LIST OF ABBREVIATIONS xi

LIST OF APPENDICES xiii

ABSTRAK xiv

ABSTRACT xv

CHAPTER 1 INTRODUCTION 1

1.1 General Introduction 1

1.2 Problem Statement 3

1.3 Objectives of the Study 4

1.4 Thesis Originality 4

1.5 Thesis Overview 6

CHAPTER 2 LITERATURE REVIEW 8

2.1 Surface Plasmon Resonance (SPR) 8

2.1.1 Principle of SPR 8

2.1.2 Localized Surface Plasmon Resonance (LSPR) 11

2.1.3 Materials for SPR 13

2.2 Enhancement of Au and Ag coated SPR Sensor with 2D Nanomaterials 14

2.3 Fiber Optics SPR-based Sensor 17

2.3.1 Introduction to Fiber Optics Sensor 17

2.3.2 U-bent Fiber Sensor 18

2.3.3 D-Shaped Fiber Sensor 20

2.3.4 Optical Fiber SPR-based Sensor for Refractive Index and Salinity Level Sensing ... 21

2.4 Review on POF SPR-based sensor ... 23

2.4.1 Advantages of POF ... 23

2.4.2 Geometry of POF SPR Based Sensor ... 24

2.4.3 Application of POF SPR Based Sensor ... 26

CHAPTER 3 METHODOLOGY ... 28

3.1 Introduction ... 28

3.2 Fabrication of POF probe ... 29

3.2.1 Preparation of Fiber Part I: Preparation of U-bent Fiber ... 29

3.2.2 Preparation of Fiber Part II: Preparation of D-shaped Fiber ... 30

3.2.3 Deposition of Materials ... 31

3.2.3(a) E-beam Deposition ... 31

3.2.3(b) Drop-Casting of $SnSe_2$ ... 32

3.3 Characterization for Fiber Optics ... 34

3.3.1 Microscopic image of D-shaped fiber ... 34

3.3.2 Transmission of Light in Fiber with Increment of Polishing Depth ... 34

3.4 Characterization of Materials ... 34

3.4.1 Field Emission Scanning Electron Microscopy (FESEM) ... 34

3.4.2 Atomic Force Microscope (AFM) ... 35

3.4.3 Ultraviolet-visible (UV-Vis) Absorption ... 36

3.4.4 MiePlot Simulation ... 36

3.5 Refractive Index Sensor ... 37

3.5.1 Stability ... 37

3.6 Salinity Sensor ... 38

CHAPTER 4 RESULTS AND DISCUSSION ... 39

4.1 Introduction ... 39

4.2 Comparison Method of Polishing ... 39

4.2.1 Transmission of Uncoated fiber ... 39

4.3 Silver Deposition ... 44

4.3.1 FESEM ... 44

4.3.2 AFM ... 47

4.3.3 UV-Vis Absorption Analysis ... 49

4.3.4 Transmission of Coated Fiber ... 51

4.3.4(a) Thickness Optimization ... 51

4.4 Sensor Performance ... 53

4.4.1 Sensitivity ... 53

4.4.1(a) Refractive Index Sensor ... 53

4.4.1(b) Salinity Level Sensor ... 56

4.4.2 Sensor Stability for RI and Salinity Level Sensor ... 58

4.5 Enhancement of the Ag Coated Fiber Probe Sensor with $SnSe_2$ layer ... 61

4.5.1 FESEM Image of Ag/$SnSe_2$ ... 61

4.5.2 UV-Visible Absorption of Ag/$SnSe_2$ ... 62

4.5.3 RI Sensing ... 63

4.5.3(a) Sensitivity ... 63

4.5.3(b) Stability ... 65

4.5.4 Salinity Sensing ... 67

4.5.4(a) Sensitivity ... 67

4.5.4(b) Stability ... 68

4.6 Performance Comparison Between Previous Study and This Research ... 70

CHAPTER 5 CONCLUSION AND FUTURE RECOMMENDATIONS ... 72

5.1 Conclusion ... 72

5.2 Recommendations for Future Research ... 73

REFERENCES **74**

APPENDICES

LIST OF PUBLICATIONS

LIST OF TABLES

Page

Table 2.1	Application of 2D nanomaterials in SPR sensor	16
Table 2.2	Geometries of POF SPR sensor	26
Table 2.3	Applications of POF sensors in various industries	26
Table 3.1	Parameters used during E-beam deposition in this research	32
Table 3.2	List of saline liquids for salinity level sensor	38
Table 4.1	Overall FESEM result for Ag with different thickness	46
Table 4.2	AFM Roughness	48
Table 4.3	Sensitivity analysis of POF probe sensor towards salinity level	58
Table 4.4	Stability analysis of polished POF coated with Ag film	61
Table 4.5	Sensitivity analysis of POF coated with Ag/$SnSe_2$ towards RI sensing	65
Table 4.6	Stability results for Ag/$SnSe_2$ POF fiber probe in RI sensing	66
Table 4.7	Sensitivity results of Ag/$SnSe_2$ coated POF probe in salinity sensing	68
Table 4.8	Stability results of Ag/$SnSe_2$ POF probe sensor for salinity sensing	70
Table 4.9	Performance of different types of POF-SPR sensor	71

LIST OF FIGURES

Page

Figure 2.1 (a) Otto (b) Kretschmann configuration (Fendi et al., 2023) 9

Figure 2.2 Prism Coupling SPR sensor (Fendi et al., 2023)..............................11

Figure 2.3 LSPR in AuNPs (Fendi et al., 2023) 12

Figure 2.4 The construction of LSPR in biosensor (Hassan et al., 2021) 13

Figure 3.1 Flowchart of the experimental steps of this research 28

Figure 3.2 U-bent fiber preparation 29

Figure 3.3 Wheel grinding polishing method 30

Figure 3.4 The Figure “8” motion in abrasive polishing method (Nunzio Cennamo et al., 2013) 31

Figure 3.5 Process of drop-casting of $SnSe_2$ 33

Figure 3.6 The setup for the fiber probe sensor..37

Figure 4.1 Microscopic image of (a)(i)(ii) 15 minutes polished fiber (b)(i)(ii) 30 minutes polished fiber (c)(i)(ii) 45 minutes polished fiber 40

Figure 4.2 Microscopic image of (a)(i)(ii) 10 strokes polished fiber (b)(i)(ii) 15 strokes polished fiber (c)(i)(ii) 20 strokes polished fiber.............41

Figure 4.3 Graph of (a-b) Polishing Time vs Diameter with transmission 43

Figure 4.4 Graph of (a-b) Strokes vs Diameter with transmission......................43

Figure 4.5 FESEM Image and Histogram (a) 5 nm (b) 10 nm (c) 20 nm (d) 30 nm...45

Figure 4.6 AFM imaging of Ag with a thickness of (a) 5 nm (b) 10 nm (c) 20 nm (d) 30 nm 48

Figure 4.7 UV-Visible Absorption of different thicknesses of Ag......................50

Figure 4.8 Mie simulation of UV-Vis absorption of Ag 51

Figure 4.9 Transmission of POF probe coated with various thicknesses of Ag for (a) wheel grinding method (b) abrasive polished method 53

Figure 4.10 Transmission of fiber probe in RI sensor for (a) 30 minutes polished POF (coated with 5 nm Ag film) (b) 15 strokes polished POF (coated with 5 nm Ag film)..55

Figure 4.11 Sensitivity analysis with increasing thickness of Ag of each probe for (a) wheel grinding method (b) abrasive polishing method...........56

Figure 4.12 Transmission of fiber probe in salinity sensor for (a) 30 minutes polished POF (coated with 5 nm Ag film) (b) 15 strokes polished POF (coated with 5 nm Ag film)..57

Figure 4.13 Stability of 15 strokes polished POF probe (coated with 5 nm Ag film) for (a) RI sensing (b) Salinity sensing......................................59

Figure 4.14 Stability of Ag coated 30 minutes polished POF probe (coated with 5 nm Ag film) for (a) RI sensing (b) Salinity sensing........................60

Figure 4.15 FESEM image of $Ag/SnSe_2$ 62

Figure 4.16 UV-Visible absorption of $Ag/SnSe_2$ 63

Figure 4.17 Transmission of $Ag/SnSe_2$ POF probe in RI sensor for (a) 30 minutes polished POF (b) 15 strokes polished POF 65

Figure 4.18 Stability analysis for Ag/SnSe2 coated POF in RI sensor for (a) 30 minutes polished POF (b) 15 strokes polished POF 66

Figure 4.19 Transmission results of $Ag/SnSe_2$ coated POF probe in salinity sensing for (a) 30 minutes polished POF probe (b) 15 strokes polished POF probe..68

Figure 4.20 Stability analysis of $Ag/SnSe_2$ coated POF probe in salinity sensing for (a) 30 minutes polished fiber (b) 15 strokes polished fiber 70

LIST OF SYMBOLS

a	Radius of fiber core
k_{spp}	Wave vector between metal and dielectric layer
ε_{metal}	Dielectric function for metal
$\varepsilon_{dielectric}$	Dielectric function for dielectric medium
k_o	Wave vector for free space
k_x	Wave vector for glass-metal dielectric layer
θ_{inc}	Incident angle
n_{glass}	Refractive index of glass prism
R	Bending radius of probe
ρ	Height of the entrance at bent region
n_1	Refractive index of core
n_2	Refractive index of cladding
S_{RI}	Refractive Index Sensitivity
S_{CONC}	Concentration Sensitivity
ΔI	Changes of intensity
ΔRI	Changes of refractive index
$\Delta\%/mL$	Changes of percentage of NaCl per milliliter

LIST OF ABBREVIATIONS

2D	Two-dimensional
AFM	Atomic Force Microscopy
Ag	Silver
AgNPs	Silver nanoparticles
Al	Aluminum
Au	Gold
AuNIs	Gold Nanoislands
AuNPs	Gold Nanoparticles
AuNR	Gold Nanorod
AuNWs	Gold Nanowires
CFU	Colony-Forming Units
CNT	Carbon Nanotubes
COFs	Covalent Organic Frameworks
Cu	Copper
DNA/RNA	Deoxyribonucleic Acid/Ribonucleic Acid
FESEM	Field Emission Scanning Electron Microscopy
FO	Fiber Optics
FO-SPR	Fiber Optics – Surface Plasmon Resonance
FOM	Figure Of Merit
FWHM	Full Width at Half Maximum
GO	Graphene Oxide
INOR	Institute of Nano Optoelectronics Research and Technology
LHDS	Layered Double Hydroxides
LSPR	Localized Surface Plasmon Resonance
LPP	Localized Plasmon Polariton
MMF	Multimode Fiber
MoS_2	Molybdenum Disulfide
$MoSe_2$	Molybdenum Diselenide
MOFS	Metal Organic Frameworks
NaCl	Sodium Chloride
PDMS	Polydimethylsiloxane

PMMA	Polymethylmethacrylate
POF	Plastic Optical Fiber
$PtSe_2$	Platinum Diselenide
rGo	Reduced Graphene Oxide
RI	Refractive Index
RMS	Root Mean Square
SMF	Single Mode Fiber
SnSe	Tin Selenide
$SnSe_2$	Tin Diselenide
SPP	Surface Plasmon Polariton
SPR	Surface Plasmon Resonance
SPW	Surface Plasmon Waves
TIR	Total Internal Reflection
TMDs	Transition Metal Dichalcogenides
TMO	Transitional Metal Oxides
USM	Universiti Sains Malaysia
UV	Ultraviolet
WS_2	Tungsten Disulfide
WSe_2	Tungsten Diselenide

LIST OF APPENDICES

APPENDIX A FIGURE OF ELECTRON BEAM EVAPORATOR

APPENDIX B RESULTS OF TRANSMISSION

APPENDIX C FESEM IMAGE OF AG/$SNSE_2$

CIRI-CIRI PENGESANAN PLASMONIK BERSEPADU DALAM PELBAGAI KONFIGURASI PROB GENTIAN OPTIK PLASTIK

ABSTRAK

Memanfaatkan fenomena Surface Plasmon Resonance (SPR), penyelidik masa kini menyepadukan prinsip tersebut dengan alatan berkuasa dalam industri sensor optik, seperti gentian optik (FO). Gentian optik plastik (POF) menjadi pilihan yang disukai kerana fleksibilitinya, ketahanannya, dan kos yang efektif. Sensor SPR konvensional mempunyai konfigurasi kompleks dan sensitivity rendah, oleh itu, penyelidikan ini mengubah suai POF yang biasa kepada POF bentuk D dan U, kemudian menggabungkan ia dengan SPR bagi mengoptimumkan sensor tersebut. POF disalut dengan perak (Ag) sebagai bahan plasmonik dan diuji dalam penderiaan indeks biasan (RI) dan tahap kemasinan sesuatu cecair. Bagi melanjutkan kajian, gentian disalut dengan tin diselenide ($SnSe_2$) pada lapisan Ag untuk meningkatkan prestasi sensor dari segi sensitviti dan kestabilan kerana ia mempunyai nisbah permukaan-ke-isipadu yang besar. Prestasi sensor dikaji dengan mengukur perubahan keamatan dan mengira sensitiviti bagi sensor RI dan tahap kemasinan. Kestabilan dikaji bagi memastikan sensor tersebut stabil. Keputusan menunjukkan gentian dengan salutan 5 nm Ag yang digilap oleh teknik pengisar roda mempunyai sensitiviti tertinggi iaitu 32300 a.u/RIU, manakala, gentian yang digilap secara manual lebih stabil. Salutan $SnSe_2$ pada prob bersalut Ag menyebabkan kestabilan dan sensitviti lebih rendah iaitu 23232 a.u/RIU, membuktikan bahawa penyelidikan yang lebih lanjut diperlukan bagi memahami penggabungan $SnSe_2$ dalam sensor SPR. Tesis ini menyumbang kepada kemajuan sensor plasmonik berasaskan POF dan berpotensi digunakan dalam pelbagai industri.

SENSING CHARACTERISTICS OF PLASMONICS INTEGRATED IN VARIOUS CONFIGURATIONS OF PLASTIC OPTICAL FIBER PROBE

ABSTRACT

Leveraging the phenomenon of Surface Plasmon Resonance (SPR), researchers nowadays integrate its principle with powerful tools in the optical sensing industry, such as fiber optics (FO). Plastic optical fiber (POF) has become a favourable choice due to its flexibility, durability, and cost-effectiveness. Conventional SPR sensors suffer from complex configuration and low sensitivity, thus, this study modified a standard POF into U-bent D-shaped and integrated it with SPR sensor with the aim of optimizing the SPR sensor. The POF was coated with silver (Ag) as plasmonic material, then tested in refractive index (RI) and salinity level sensing for a certain liquid. To further the study, the fiber was then coated with tin diselenide ($SnSe_2$) onto Ag layer to enhance the performance of the sensor in terms of sensitivity and stability due to its characteristic, which is large surface-to-volume ratio. The sensing performance was characterized by measuring the intensity changes and calculating sensitivity for the RI and salinity level sensor. The stability of the sensor was studied to ensure it provided a stable performance. Results showed that the wheel grinding polished fiber with 5 nm Ag coating provided the highest sensitivity, which is 32300 a.u/RIU, while abrasive polished fiber with 5 nm Ag coating exhibited more stability. Surprisingly, the deposition of $SnSe_2$ onto Ag coated POF probe led to lower stability and sensitivity, which is 23232 a.u/RIU, suggesting that further research is needed to fully understand the incorporation of $SnSe_2$ in SPR sensor. This thesis contributes to the advancement of POF-based plasmonic sensors and has the potential to be used in diverse industries.

CHAPTER 1

INTRODUCTION

1.1 General Introduction

Surface Plasmon Resonance (SPR) sensors have become an effective technology for sensing applications, including biomedical (S. Liu et al., 2021), environmental (Teng et al., 2024), and food industry (Vikas et al., 2020) because of their excellent performance such as high sensitivity (M. N. Sakib et al., 2019), real-time monitoring capabilities (M. N. Sakib et al., 2019), and versatility (Takemura, 2021). The conventional SPR sensor with a prism-coupling configuration is considered bulky and costly. Therefore, different kinds of technologies were introduced to improve SPR sensors, and one of the most significant ways is by using fiber optics. Fiber Optics-SPR (FO-SPR) sensor was proven to be a good option as it offers benefits like compact in size, good mobility, cost-effectiveness, high sensitivity, and many more (Semwal & Gupta, 2019).

Modifying the straight optical fibers into different geometries like U-bent, D-shaped, tapered, and others can enhance the performance of the FO-SPR sensor. A previous work mentioned that the design for simple and compact sensors could be obtained by fabricating a U-bent fiber probe while achieving high sensitivity sensor performance (Rajamani et al., 2019). Meanwhile, D-shaped geometry improves light coupling between Surface Plasmon Polariton (SPP) and core to enhance the SPR phenomenon, thus increasing the sensitivity of their proposed blood component sensor (S. Liu et al., 2021). In recent years, the performance of polished U-bent fiber has been studied due to its unique mechanism and potential to improve sensor performance. Teng et al. studied a polished U-bent fiber where the fiber was coated with gold (Au) and polydimethylsiloxane (PDMS) (Teng, Shao, et al., 2022). It was proven that U-bent polished fiber can be used in diverse applications due to its high sensitivity.

The choice of material coated on the fiber is also important in constructing SPR sensor, as the material will be interacting with the light signal. To excite Surface Plasmon Particle in SPR sensor, the plasmonic material must be optimal with the application itself and the famous plasmonic materials reported in these few years were gold (Au), silver (Ag), Copper (Cu), and many more. Apart from that, there were new trends of materials coated onto fiber which are integrating plasmonic material with other material such as the combination of plasmonic materials like Ag/Au (Chang et al., 2018), the combination of plasmonic material with nanomaterials like Au/AuNPs (Niu et al., 2019), Ag/MoS_2 (N. H. Kim et al., 2019), Au/ SnSe/graphene (Sathya et al., 2022), and many more. By combining these materials, the performance of the SPR sensor can be enhanced due to the enhancement of the interaction between materials and the light signal. In recent years, two-dimensional (2D) nanomaterials such as MoS_2, $MoSe_2$, graphene, SnS_2, and $SnSe_2$ are one of good candidates to be applied in SPR sensors. $SnSe_2$ is said to have large surface-to-volume ratio (M. Chen et al., 2018) that can enhance the interaction between the material and target analyte while being cost-effective, environmentally friendly, and having high carrier mobility (Y. Wang et al., 2017). Given all of these advantages, there is still limited research done on $SnSe_2$ in the SPR sensor.

Thus, in this research, the U-bent D-shaped probe fiber sensor was optimized by studying the geometry and structure of the fiber probe, plasmonic coating thickness, and incorporation of $SnSe_2$ onto the plasmonic material layer to achieve high sensitivity and stability sensor performance.

1.2 Problem Statement

SPR sensors have been widely used in various detection due to their high sensitivity to their surroundings (Zakaria et al., 2021). Conventional SPR is in a bulky form involving a prism-coupled configuration, which can be considered as complex due to the need for precise angle measurement of prism rotation (Semwal & Gupta, 2019a). To address these drawbacks, FO-SPR sensors were introduced as they offer advantages like remote sensing, being easy to handle, compact, immune to electromagnetic interference, and cost-effective in manufacturing (Zakaria et al., 2021). Over the years, different kinds of fiber have been employed, including U-bent, D-shaped, tapered, grating, and many more, to enhance the performance of the fiber probe sensor compared to a straight fiber probe.

These few years, most of the reported FO sensors have been using glass optical fiber sensor. The glass optical fiber sensor is said to be more fragile and costly compared to plastic optical fiber (POF) (Khonina et al., 2023), where it can be troublesome for the users. Therefore, it makes glass optical fiber less practical to be used in various applications including the most basic application, refractive index (RI) sensor. There are few works reported that the glass optical fiber was not effective to be applied, for example, a study review by Gierej et al., where they mentioned that glass optical fiber is brittle, which can break and shatter easily, making it not suitable to be used in biomedical applications (Gierej et al., 2021). Therefore, this study wanted to introduce a more reliable sensor to be used in different applications, like RI and salinity level sensors.

Apart from that, the construction of SPR that only involves plasmonic material was reported to have lower sensitivity compared to hybrid coated material. For instance, Niu et al. in their work stated that their proposed sensor with additional nanoparticle, AuNPs, achieved a sensitivity of 760 nm/RIU higher than the sensor with only Au film (Niu et al., 2019). Sathya et al. also mentioned that their simulation of their proposed prism SPR sensor with the addition of SnSe on Ag/graphene layer led to a higher sensitivity. Therefore, there is a need to incorporate another layer of material onto the plasmonic layer to enhance the sensitivity of the sensor.

In this thesis, the straight POF was modified into U-bent and polished it to become a D-shaped fiber in order to construct a probe sensor. The probe was then coated with a plasmonic material, which is Ag, to initiate the SPR phenomenon and $SnSe_2$ was coated onto Ag to enhance the performance of the sensor. The performance of the fiber probe sensor was determined through Refractive Index (RI) sensing and salinity sensing.

1.3 Objectives of the Study

The objectives of this study are:

1. To modify the standard POF into the D-shaped U-bent fiber SPR probe using wheel grinding and abrasive polishing method.
2. To investigate the RI and salinity level sensor performance for a certain liquid in terms of sensitivity and stability using the D-shaped U-bent fiber SPR probe.
3. To assess the enhancement of sensing performance in terms of sensitivity and stability of the sensor prior to the incorporation of $SnSe_2$ into D-shaped U-bent fiber coated with Ag/$SnSe_2$.

1.4 Thesis Originality

POF SPR based sensors have been studied a lot to improve their performance from time to time. Implication of POF in SPR sensor contributed in enhancing the performance of the sensor, especially when the structure of the fiber was modified to adjust with the compatibility of the application. There were a few elements in this study that show the originality of this research, which was inspired by previous research. The originalities of this research are:

1. Modification of a standard POF into different geometries and integrating it with SPR sensors for different applications, such as RI sensor and salinity sensor. The proposed sensor was designed to be in a U-shaped D-bent POF coated with Ag as plasmonic material. The bent region and narrow diameter lead more light to leak, thus promoting more interaction between light and the material coated on the fiber. Therefore, this design was meant to enhance the sensitivity of the sensor. Research by Teng, Shao et al in 2022 inspired this study, where they modified a straight optical fiber into a double-side polished U-bent fiber. This research stated that their proposed sensor is easy to fabricate and compact, while achieving high sensitivity (Teng, Shao, et al., 2022). As this thesis was inspired by Teng, Shao et al., the proposed design of the sensor from this thesis, which deploys POF, has not yet reported in any journal. Therefore, this thesis claims that the design of the sensor itself is the novelty of this research study. Besides, there is no study that compares the method of polishing fiber into D-shaped yet, thus, the comparison between the wheel grinding polishing method and abrasive polishing method is the novelty of this research as well.

2. The application of the proposed sensor is applied in RI and salinity level sensing applications. Most of the reported FO-SPR sensors were made up from glass optical fiber, yet the proposed sensor from this thesis has never been used

in any application. Thus, by applying the proposed sensor, it will contribute in providing new insights into POF studies.

3. The incorporation of $SnSe_2$ onto Ag layer. This was meant to enhance the performance of the sensor in terms of sensitivity due to its characteristic, which is large surface-to-volume ratio, which can enhance the interaction between materials and the target analyte (M. Chen et al., 2018). Currently, there are limited sources that study the deployment of $SnSe_2$ with Ag. In addition, there is no study reported for the deployment of Ag/$SnSe_2$ in POF SPR sensor.

1.5 Thesis Overview

In this thesis, there are five chapters documenting U-bent D-shaped fiber probe SPR sensors in various applications, including RI sensors and salinity sensors.

Chapter 1 explains the introduction and background of this study from general views. Then, this chapter states the problem statement, objectives, research questions, and novelty of this study.

Chapter 2 discussed the literature review on the principle of SPR and fiber optics, including different configurations like U-bent fiber and D-shaped fiber, the fiber optics sensor with different configurations, and current applications of the optical fiber SPR-based sensor.

Chapter 3 focused on the methodology for fabricating the U-bent D-shaped fiber probe, deposition of Ag as plasmonic material, deposition of $SnSe_2$, characterization of the materials, and finally, performance testing for each application.

Chapter 4 discussed the outcome of the project, which begins with the characterization of the fiber and the material deposited, followed by the results of various tests of the sensor.

Lastly, Chapter 5 presents the conclusion of this whole project along with future recommendations. The appendices of this research were presented after Chapter 5 and references.

CHAPTER 2

LITERATURE REVIEW

2.1 Surface Plasmon Resonance (SPR)

2.1.1 Principle of SPR

SPR refers to the excited charge density oscillation along with the metal-dielectric interface, with the permittivity of opposing signs (Ho et al., 2017). This phenomenon relates to the resonance of a strong electromagnetic field oscillation at the interface of a nanometal film and dielectric medium with p-polarized incident light. This results in a dark band profile in the light reflectivity at an incident angle and specific wavelength (Prabowo et al., 2018). The specific wavelength, called resonance wavelength, depends on the dielectric material's refractive index (Semwal & Gupta, 2019a). Furthermore, Surface Plasma Waves (SPW) or SPP can be created when the orientation of the electric field vector of an incident light complements the motion of free electrons in the metal. It is controlled by boundary restrictions connected with the material and structural considerations, and thus efficient coupling with large energy as guided electromagnetic waves along the interface can happen (Ho et al., 2017). SPR sensor is known for their high sensitivity and different types of design (Y. Zhao et al., 2019). Additionally, the prism-coupled sensor is the earliest type of sensor discovered by Otto and then improved by Kretschmann. According to Zhao et al., the prism-coupled SPR in Otto configuration was based on attenuated total reflection. The Kretschmann configuration then improved it as the analytes separated the prism and plasmonic metal layer, leading to a complex design (Y. Zhao et al., 2019). Figure 2.1 (a) and Figure 2.1 (b) display the Otto and Kretschmann configuration design. Otto and Kretschmann's configuration have been widely used in SPR-based sensors. Nevertheless, the drawback of these configurations is the large and complex design.

Thus, the design of the SPR sensor has been upgraded to enhance its performance. For instance, as was mentioned by Zhao et al., a few designs are created, such as prism couple sensor, grating coupled sensor, optical fiber coupled sensor, and waveguide coupled sensor (Y. Zhao et al., 2019).

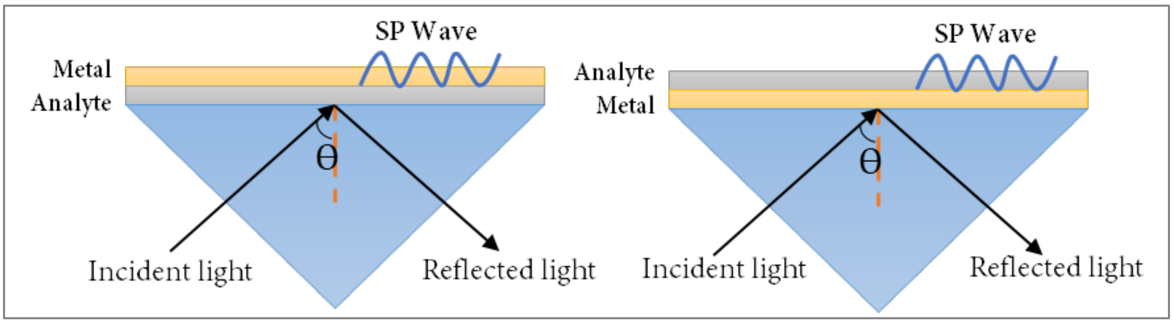

Figure 2.1 (a) Otto (b) Kretschmann configuration (Fendi et al., 2023)

SPR occurs when light irradiates the metal-to-medium interface. It will resonate with the SPW to induce energy transfer and causes the light intensity to rapidly decrease from resonant wave valleys at a specific wavelength (Jing et al., 2019; Luo & Wang, 2021; Q. Wang et al., 2019). The resonance condition varies when a metal surface changes the RI, causing the resonance wavelength to move. As a result, the movement of the resonance trough produced by a change in the external medium's RI can be employed for sensing (Luo & Wang, 2021). Moreover, SPW can be formed between a dielectric layer and a metal layer as the evanescent wave can penetrate through the metal layer. Surface plasmon oscillates and propagates along the boundary between a dielectric medium and a thin metal film. The wave vector (k_{spp}) between metal and dielectric layer can be written as (Mukhtar et al., 2013):

$$k_{spp} = k_0 \sqrt{\frac{\varepsilon_{metal}\varepsilon_{dielectric}}{\varepsilon_{metal} + \varepsilon_{dielectric}}} \qquad (2.1)$$

where ε_{metal} is the dielectric function for metal, $\varepsilon_{dielectric}$ is the dielectric function for dielectric medium, and k_0 is the wave vector for free space of the optical wave. It can be calculated using the formula (Mukhtar et al., 2013):

$$k_0 = \frac{2\pi}{\lambda_0}. \quad (2.2)$$

The incident light's energy can be firmly linked from photons onto the surface plasmon wave, which dissipates by heat dissipation along the propagation route during SPR. The relationship between k_x and the angle of incident light can be described by the equation (Mukhtar et al., 2013):

$$k_x = k_0 n_{glass} \sin\theta_{inc} \quad (2.3)$$

where n_{glass} is the index of refraction of the glass prism and θ_{inc} is the incident angle. In a glass-metal-dielectric system, the requirements for surface plasmon excitation at the metal-dielectric layers interface are indicated by:

$$k_x = k_{spp}. \quad (2.4)$$

Resonance is obtained by matching the projection of the incident light's wave vector in the direction of the interface with the wave vector of the surface plasmon oscillations, as indicated in equation (2.4). The value of k_x can be calculated using a prism with a dielectric constant greater than 1 and an incidence angle greater than the critical angle. The reflectance significantly decreases absorption when the incident light meets the resonance requirement. Figure 2.2 displays the total internal reflection (TIR) in the prism coupling SPR sensor.

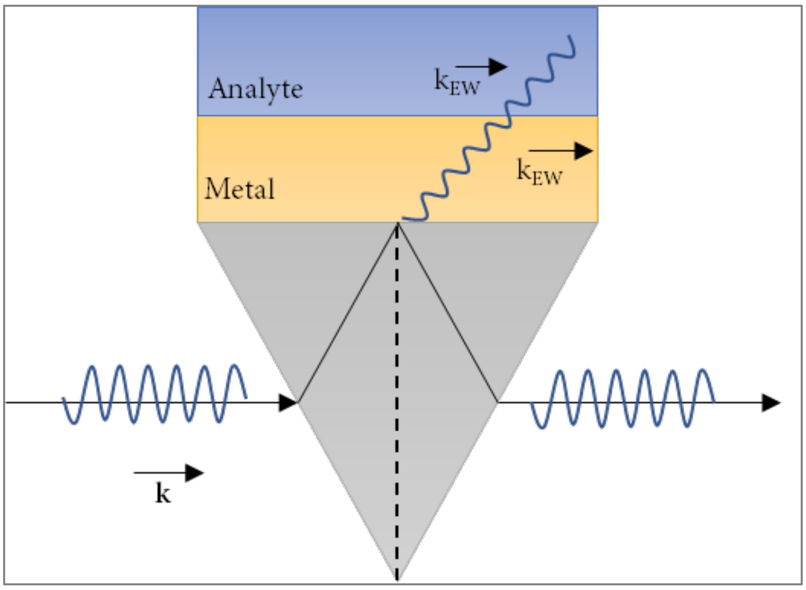

Figure 2.2 Prism Coupling SPR sensor (Fendi et al., 2023)

2.1.2 Localized Surface Plasmon Resonance (LSPR)

Compared to the SPR phenomenon excited by a thin metal film, LSPR is regulated to smaller particles called nanoparticles with a size range from 1 nm to 100 nm. It happens when a light wave is trapped within conductive nanoparticles smaller than the wavelength of light. The interaction of incident light with surface electrons in a conduction band causes this phenomenon (Xu & Geng, 2021). It is observed in metal nanoparticles where electromagnetic light hits the metal nanoparticles, resulting in the interaction between the electric field and free electrons. This causes them to be distinct from the metal core. The repulsive force between electrons makes them travel in opposite directions, causing them to oscillate and excite the LSPR. Strong light absorption can be induced via LSPR excitation (Das et al., 2020). Few parameters can affect the resultant wavelength position of the LSPR absorption bands, such as size, shape, interparticle distance or aggregation state of the nanoparticles, composition, and the dielectric constant of the surrounding medium (Razali et al., 2020; Rivero et al., 2018). The function of LSPR is implemented to detect the RI changes in a small area as it deals with smaller volumes. When the SPP and the Localized Plasmon Polariton

(LPP) exist simultaneously, they will pair to generate a localized electromagnetic field enhancement (Niu et al., 2019). As it enhances the electromagnetic field, it can also maximize the optical extinction of the metal nanoparticles. According to Bai et al., LSPR can increase the time for optical extinction for AuNPs more than 1,000 times stronger than typical organic molecules, where it can enrich the photothermal conversion efficiency, light absorption, and photochemistry conversion of AuNPs (Bai et al., 2020). Figure 2.3 illustrates the phenomenon of LSPR of AuNPs.

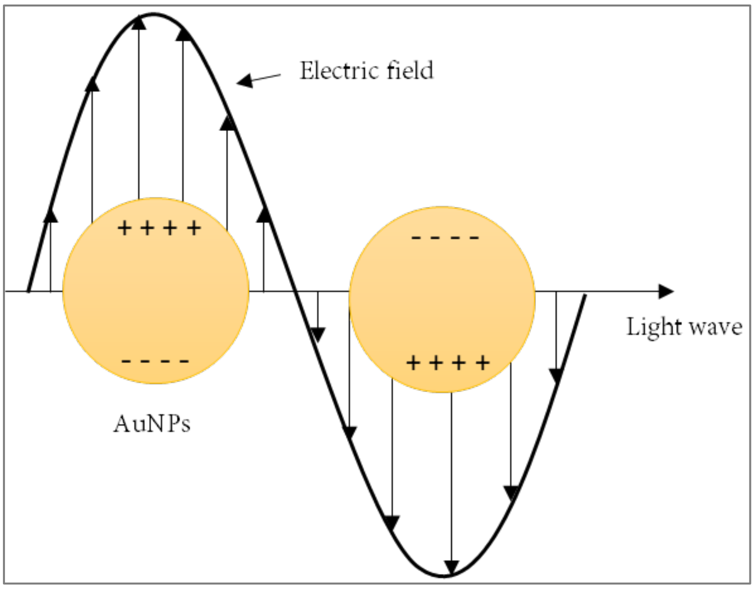

Figure 2.3 LSPR in AuNPs (Fendi et al., 2023)

LPSR sensors have been used in a few industries, such as clinical uses (Xu & Geng, 2021), virus detection (E. J. Kim et al., 2021), food safety, and environmental monitoring (Fadzil & Mukhtar, 2015). According to Qiu et al., among other sensing techniques for biosensing, LSPR applies to different types of analytes of clinical interest. This is due to local variations, such as RI change and molecule binding detected with high-sensitivity LSPR sensing systems (Qiu et al., 2020). As a result, LSPR is an excellent choice for detecting microscale and nanoscale analytes in real time and without the need for labels. For example, Hassan et al. stated that LSPR biosensor is utilized for virus detection (Hassan et al., 2021). Figure 2.4 portrays the construction of the LSPR biosensor.

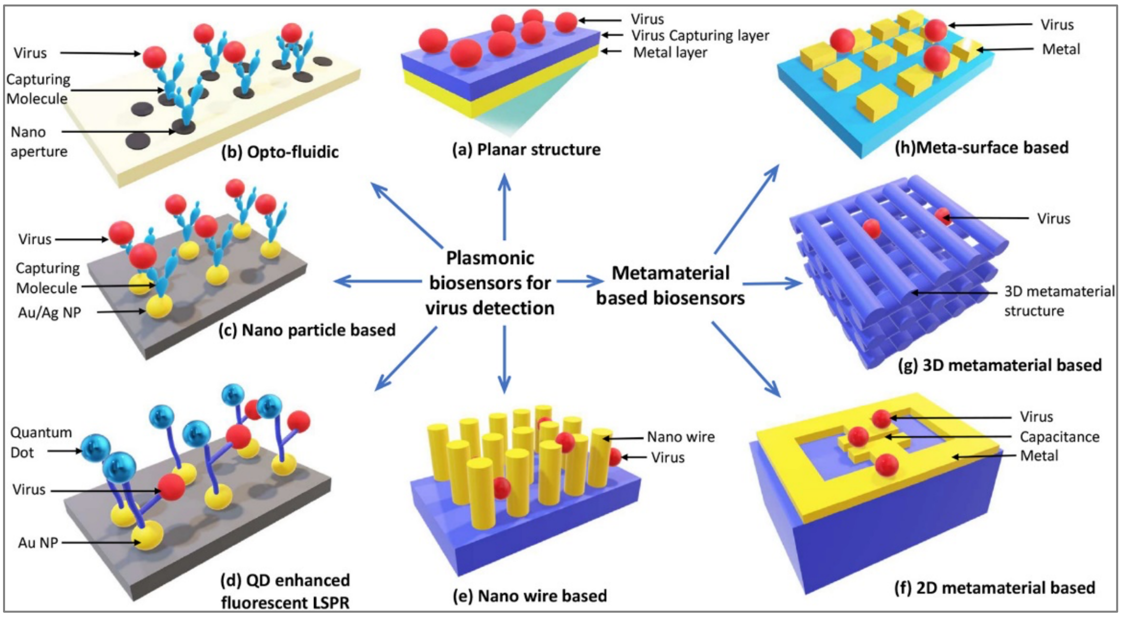

Figure 2.4 The construction of LSPR in biosensor (Hassan et al., 2021)

2.1.3 Materials for SPR

The construction of the SPR sensor must be equipped with plasmonic materials to trigger the SPR phenomenon and perhaps other materials to support sensing action and enhance performance. In an optical fiber sensor, materials are coated on the fiber to enhance the performance including increasing sensitivity of the sensor. An early configuration of SPR usually uses a single layer of a plasmonic thin film that can excite the SPR effect. Nevertheless, as time passes, numerous research has been conducted, resulting in the use of multilayer materials known as hybrid material instead of a single plasmonic thin film. The commonly used materials in SPR sensors include Au (N. Sakib et al., 2021), silver (Ag) (E. J. Kim et al., 2021), Copper (Cu) (S. Chen & Lin, 2019), and Aluminum (Al) (Ibrahim et al., 2019). The latest design of the SPR sensor uses nanoparticles instead of a thin film such as AuNPs (Huang et al., 2021) to excite the SPR effect, as nanoparticles also result in excellent performance. Few improvements were made by previous research on plasmonic materials, where they combine a single plasmonic thin film layer with other materials like graphene (Moznuzzaman et al., 2021), Graphene Oxide (GO) (E. J. Kim et al., 2021), and hydrogel (Y. Zhao et al., 2018) to enhance performance. It is stated by Niu et al. that the methods that can enhance the sensitivity of detection include two aspects: one is to add a dielectric layer on the sensor's surface to increase the load of the object to be measured, such as dopamine and reduced graphene oxide (rGO). The other is to use metal nanoparticles, such as AuNPs, gold nanorods (AuNR), magnetic nanoparticles, and conical nanoparticles (Niu et al., 2019). In addition, a new form of nanoparticles was recently implemented to excite the LSPR effect, such as gold nanowires (AuNWs) (Z. Zhao & Wang, 2022), Au nanosphere (Z. Zhao & Wang, 2022), gold nanoisland (AuNIs) (Qiu et al., 2020), and AuNR (Z. Zhao & Wang, 2022).

2.2 Enhancement of Au and Ag coated SPR Sensor with 2D Nanomaterials

Traditional SPR sensors consist of plasmonic materials such as Au and Ag to excite surface plasmon and only relies on the material to enhance the performance of the sensor. Recently, the trend of enhancing the performance of SPR sensors has focused on including additional materials onto plasmonic material. This innovation can improve the sensitivity and widen the range of detectable analytes. Different materials were added such as noble metals like Au, Ag, and Cu, nanomaterials like AuNPs, graphene, and many more. The famous trend in this current time is integrating 2D nanomaterials such as graphene, black phosphorus, 2D metal carbides and nitrides (MXenes), transition metal dichalcogenides (TMDs), and layered double hydroxide. 2D nanomaterials are materials that have a thickness of a few nanometers which consist of one or few layers of atoms (Tufail et al., 2024). 2D nanomaterials are classified into three categories, which are organic, inorganic, and hybrid. Examples of organic 2D nanomaterials are covalent organic frameworks (COFs), polymer nanosheets, sequence-defined 2D nanomaterials derived from proteins, DNA/RNA, peptides, and peptoids. Inorganic 2D nanomaterials consist of monolayers of carbon atoms like graphene, transitional metal oxides (TMOs), TMDs, MXenes, monoelemental 2D semiconductors, layered silica, and layered double hydroxides (LHDs). Meanwhile, the hybrid 2D nanomaterials are metal organic frameworks (MOFs) (Murali et al., 2021).

Graphene-based nanomaterial is one of the famous 2D nanomaterials used in the SPR sensor industry. It has a high surface-to-volume ratio, which leads to high adsorption ability and increases the interaction between materials (Sathya et al., 2022). Besides, graphene possesses effective charge transfer, which can increase the sensitivity due to the strong coupling effect from graphene (Xi et al., 2020). However, graphene can also reduce the accuracy of the sensor, as mentioned in a study by Rouf and Haque in 2021, where they proposed a SPR sensor coated with Ag, graphene, and Molybdenum diselenide ($MoSe_2$). They found out that graphene requires a large number of $MoSe_2$ layers to obtain effective light energy transfer, which can decrease the detection accuracy, and increase the electron energy loss and full width at half-maximum (FWHM) (Rouf & Haque, 2021). Black phosphorus is also a strong competitor as it provides good optoelectronic properties, direct bandgap, and high carrier mobility (Rahman et al., 2022). Research proved that using black phosphorus with other layers of materials can enhance the performance. For instance, A. Srivastava et al. obtained a maximum sensitivity of 190.220/RIU theoretically by using black phosphorus, Mxene-$Ti_3C_2T_x$, and TMDs (Srivastava et al., 2020).

On the other hand, TMDs like Molybdenum disulfide (MoS_2), Tin diselenide ($SnSe_2$), Tin selenide (SnSe), Platinum diselenide ($PtSe_2$), and others are the rising 2D nanomaterials used in SPR sensor. TMDs are good candidates for enhancing sensor performance due to their flexibility, large surface area, atomically thin, chemically stable, moderate carrier mobility, and optoelectrical properties that depend on the layer (AlaguVibisha et al., 2020). Kumar et al. obtained a high sensitivity performance from their proposed sensor, the values achieved 271.25 deg/RIU and 290.714 deg/RIU for cervical and blood cancer cells based on numerical data. They claimed that with the addition of MoS_2, the highest sensitivity is achieved, and MoS_2 and $MoSe_2$ are perfect options for enhancing SPR sensitivity (Kumar et al., 2024). N.H Kim et al. also discovered that by including TMDs, which is MoS_2 on Ag, the sensitivity was improved by 125% (N. H. Kim et al., 2019). The newly discovered TMDs is $SnSe_2$, where, nowadays, many research has been done to study the properties of $SnSe_2$. D'Olimpio et al., in their study, mentioned that $SnSe_2$ has high intrinsic electron mobility compared to MoS_2 and tungsten disulfide (WS_2) (D'Olimpio et al., 2022). This makes it a good candidate for the SPR sensor as it can transfer the charge faster, enhancing sensor sensitivity and response time. Wang et al. mentioned that tin dichalcogenides (SnS_2, $SnSe_2$) have drawn much attention due to their high carrier mobility and exceptional photoresponsive property. They are also cost-effective and environmentally friendly, making they are suitable to be used in optoelectronics devices (Y. Wang et al., 2017). Thus, due to their excellent properties, the deployment of $SnSe_2$ in optoelectronics devices must be studied. Table 2.1 shows the application of 2D nanomaterials in SPR sensors.

Table 2.1 Application of 2D nanomaterials in SPR sensor

Configuration	Materials	Sensitivity	FOM	Application	Ref
Prism coupling SPR	Au/WSe_2/$PtSe_2$/Black Phosphorus	200 deg/RIU	17.70 RIU^{-1}	RI sensor	(Rahman et al., 2022)
Prism coupling SPR	$PtSe_2$/Au/Blue Phosphorus/MoS_2	240.54 deg/RIU	29.23 RIU^{-1}	RI sensor	(Chowdhury et al., 2024)

Prism coupling SPR	$Ag/BaTiO_3/Ag/MoS_2$	290.714 deg/RIU	100.59 RIU^{-1}	Blood and cervical cancer detection	(Kumar et al., 2024)
Prism coupling SPR	Ag/SnSe/Blue Phosphorus/MoS_2	187 deg/RIU	24.83 RIU^{-1}	Cancerous cell detection	(Hossain et al., 2022)
Prism coupling SPR	Ag/MoS_2	Not stated but up to 125% improvement with the presence of MoS_2 layer	Not stated	Bacteria detection	(N. H. Kim et al., 2019)
Prism coupling SPR	Au/SnSe/graphene	214 deg/RIU	26.93 RIU^{-1}	RI sensor	(Sathya et al., 2022)
D-shaped fiber	Au/MoS_2/graphene	6126.25 nm/RIU	Not stated	Glucose detection	(Yu et al., 2020)
Prism coupling SPR	Au/ MXene/ WS_2/ Black Phosphorus/	190.22 deg/RIU	15.51 RIU^{-1}	RI sensor	(Srivastava et al., 2020)

2.3 Fiber Optics SPR-based Sensor

2.3.1 Introduction to Fiber Optics Sensor

Fiber Optics transmits light based on the TIR with few optical losses. It consists of a circular core and cladding surrounding the core. The value of the RI for the central core is higher compared to cladding has enabled the TIR phenomenon where light is transmitted into the fiber bent beyond the critical angle and the light that stays in the fiber will be transmitted over a vast distance (Bahl, 2019). Usually, glass or silica fiber optics are widely used in various applications. Compared to glass fiber optics, POF is more flexible, easy to handle, and cost-effective (Arcadio et al., 2023). However, Bilro and coworkers in their work mentioned that POF has more significant attenuation compared to glass fiber optics, unable to be applied in high temperature applications, which POF can withstand within the temperatures of 80°C to 100°C, limited production and lack of standardization (Bilro et al., 2012). Therefore, POF cannot be deployed in high temperature applications and needs to be studied more.

Fiber optics were fabricated in two different modes, SMF and MMF. These modes have different designs based on the amount of the paths of light transmitted. SMF, or mono-mode is designed to have only one path of light transmitted and is suitable for long-distance applications as it possesses lower attenuation and unlimited bandwidth. The multimode fiber was designed to have multiple paths of light and can be used for short-distance use. It has higher attenuation compared to the SMF. SMF possesses good performance when it comes to long-distance applications due to a narrow core. It is designed to allow only fundamental mode at a specific wavelength to propagate along its core, thus making it the best solution for modal dispersion. Although SMF possesses many advantages, it is not easy to handle, where the fiber is less flexible and becomes fragile when it is modified (Yulianti et al., 2021). Multimode on the other hand is suitable to be used in short-distance applications making it compatible with applications like biomedical, chemical, and other sensing applications. The MMF is easier to handle when engineered into different configurations as it has more flexibility.

2.3.2 U-bent Fiber Sensor

The light propagated in straight fiber is different from U-bent fiber as there is a change in the path of light transmitted. In a straight fiber, the light propagates through the core because of the TIR phenomenon at the core-cladding interface. The light is reflected into the core and propagates along the fiber as the cladding has a lower refractive index than the fiber core. As for the U-bent fiber, the propagation angle depends on the bending radius. The light propagates through a curved path, with slight bending losses and light leaks. The leaked light can propagate through the cladding and may experience attenuation due to a lower refractive index. Therefore, if a material coated on the fiber, the SPR phenomenon can occur and have better sensitivity due to more light leaking.

According to (Azkune et al., 2018), the changes in the incident angle of light propagated in U-bent fiber can be shown in equation (2.5) and (2.6):

$$\phi_1 = \sin^{-1}\left[\left(\frac{R \pm \rho}{R + a}\right)\frac{n_2}{n_1}\right] \tag{2.5}$$

$$\phi_2 = \sin^{-1}\left[\frac{R \pm \rho}{R + a}\right] \tag{2.6}$$

where R represents the bending radius of the probe, a is the radius of the fiber core, ρ is the height at the entrance if the bent region from the inner core-cladding interface. At the inner surface, the angle goes from equation (2.7) to (2.8):

$$\delta_1 = \sin^{-1}\left[\left(\frac{R \pm \rho}{R}\right)\frac{n_2}{n_1}\right] \tag{2.7}$$

$$\delta_2 = \frac{\pi}{2} \tag{2.8}$$

Previous works have been done to design better configurations for fiber optic sensors. The design involves changing the shape and diameter of the fiber itself. According to previous research, the U-bent probe provides many advantages, such as high evanescent wave absorbance sensitivity as lower modes change into higher modes, robustness, ease of fabrication, repeatability, and can be made as a point sensor (Gowri & Sai, 2016). Rajamani et al. in their work mentioned that the design for simple and compact sensors could be realized by fabricating a U-bent fiber probe while achieving high sensitivity sensor performance. Their proposed sensor with U-bent fiber is mainly to get a small footprint of the sensor to insert through a small hole, simplify the optical coupling, and avoid additional optical components such as lenses and a beam splitter (Rajamani et al., 2019). Bandaru et al. explained that the evanescent wave-based light-matter interaction at the core-medium interface of fiber is better at the bent region of U-bent fiber and allows a significant fraction of light to be available at the core surface as U-bent fiber can efficiently convert lower modes to higher modes. The numerical simulations from their work show that there is an increase in evanescent power ability for the U-bent probe (Bandaru et al., 2020).

2.3.3 D-Shaped Fiber Sensor

D-shaped or polished fiber sensor sensors are the improved FO sensors where the geometry of the fiber is modified to improve the mechanism of the fiber according to their application. The D-shaped or side-polished fiber is fabricated by minimizing the size of the fiber diameter, where a slight part of the cladding of the fiber is removed, thus enhancing the interaction between light and the surrounding medium. It produces a high evanescent field making the fiber more responsive to its surroundings (Liao et al., 2016). According to (Ying et al., 2017), when the D-shaped fiber is coated with plasmonic material, light with a specific wavelength enters the fiber and experiences the TIR. Evanescent waves will get excited and interact with plasma waves on the surface of plasmonic material. It can be described by the interface reflection coefficient r (Fresnel coefficient) as shown in the equation:

$$r_{ij} = \frac{n_i^2 k_{jy} - n_j^2 k_{iy}}{n_i^2 k_{jy} + n_j^2 k_{iy}} \tag{2.9}$$

where $k_{iy} = \frac{\omega}{c}\sqrt{n_i^2 - n_1^2 \sin^2 \theta_{inc}}$, $i = 1,2,3$ and $j = i + 1$ for any adjacent two mediums, θ_{inc} is the incident angle.

D-shaped fibers can achieve high sensitivity due to their unique mechanism that allows better light interaction between the analyte and the flattened surface of the D-shaped configuration (Stepniewski et al., 2023). For instance, a D-shaped fiber coated with Au reported a sensitivity of 3.101 a.u/RIU and linearity reaching 98% for glucose concentrations ranging from 1% to 9% (Abbas & Mahdi, 2023). However, this research demonstrated a limited range of RI concentrations, which can limit the sensor's applicability. Another research from Ren et al. reported that they chose D-shaped fiber due to its flat polished surface that is convenient for SPP excitation. Besides, the Figure of Merit (FOM) reported is 200 RIU^{-1}, which shows that the D-shaped fiber is applicable for sensing applications (Ren et al., 2022).

The D-shaped geometry of a fiber can be obtained by different methods, such as mechanical polishing and laser ablation. Mechanical polishing is a traditional technique that is simple and straightforward, as it requires simple equipment and good control of movement. There are a few ways of applying this method, for example, in a work by Amiri et al., they used a setup which is wheel grinding method setup. It was mentioned that this method is suitable for large-scale production and commercialization for sensing device applications (Amiri et al., 2023). The D-shaped can be obtained by polishing the fiber on the surface of a wheel covered with sandpaper. The polishing process can be controlled with adjusted time and speed of the wheel. The other method is by manually polishing it by hand, or known as the abrasive polishing method. The fiber was polished on the sandpaper and controlled manually by hand, for example, a work by Nunzio Cennamo et al., where this method is suitable for a low-cost production as it requires a simple procedure and equipment (Nunzio Cennamo et al., 2013). On the other hand, the newest method is by using the laser ablation method, which requires an advanced machine, such as a high-energy laser beam, to remove the fiber's surface. This method can efficiently remove the fiber's side due to good control of movement and it is free of contamination due to a non-contact process (C. Hu et al., 2021). Nevertheless, it is costly as there is a need for advanced machines and a laser for the setup.

2.3.4 Optical Fiber SPR-based Sensor for Refractive Index and Salinity Level Sensing

Recent developments in SPR-based optical fiber sensors have caused many researchers to apply them in various applications, including RI and salinity level detection. In such sensors, the surrounding medium is aqueous media with different concentrations and refractive index and the changes in these values of parameters can be detected using fiber optics SPR sensor. Usually in fiber optics sensor industry, the glass fiber optics were preferrable to be integrated with the SPR sensor as POF has higher signal attenuation compared to glass optical fiber (Zubia & Arrue, 2001), which leads to higher sensitivity. A work by Z. Zhao and Wang utilized a glass optical fiber coated with Au/AuNPs in RI sensing with an RI range of 1.31.3663 to 1.3793. Their proposed sensor achieved high sensitivity, which is up to 5174.7 nm/RIU (Z. Zhao & Wang, 2022). Apart from that, glass optical fiber has been used in salinity level sensor, for instance, Wei et al. proposed a glass fiber optics sensor to be used in detecting seawater salinity. This research tapered the fiber and coated it with Au film to enhance the performance, then achieved the sensitivity of 0.708 nm/‰ with good linearity (Wei et al., 2023).

Conversely, the POF SPR sensor offers low cost, ease of handling, and higher flexibility in this kind of application, as shown in a study by Teng, Shao et al., where they used POF to detect the changes in RI and temperature. In their study, the standard POF had been modified into double-side polished U-bent fiber and which proves the flexibility of POF, while their highest sensitivity was achieved with the value of 1258 nm/RIU (Teng, Shao, et al., 2022). As for salinity level detection, there is limited research that utilized the POF SPR sensor, nonetheless, there are a few studies that use the POF sensor without integrating it with the SPR sensor. For instance, research by Nor et al. chose POF to be used in their proposed sensor coated with carbon nanotubes (CNT) for salinity detection due to its robustness, flexibility, and large core size (Nor et al., 2023). Another research by Stupar et al. uses POF in their salinity sensor as it is low cost and easy to handle (Stupar et al., 2012). Both of these sensors provide good performance where the sensitivity is high and can be used in a long-term application, proving that POF is a good candidate to be used in salinity level sensor and even in more advanced applications.

2.4 Review on POF SPR-based sensor

2.4.1 Advantages of POF

Usually, optical fibers are made of two types of materials, which are glass and plastic. The glass fiber optics are composed of silica and offer low-loss transmission, high information carrying capacity, immunity to electromagnetic interference, and small size (Hecht, 2016). However, glass fiber is fragile and difficult to handle, making the process of fabricating and using the fiber bothersome and unsuitable for practical applications (Teng et al., 2023). On the other hand, polymer optical fiber known as plastic optical fiber has better flexibility, coupling efficiency, high numerical aperture, and low cost. It also has low-loss transmission, but compared to glass fiber optics, it possesses high signal attenuation, making it not suitable for long-distance applications (Zubia & Arrue, 2001). In addition, using POF in a sensor can help to achieve high sensitivity performance. L. Liu and coworkers reported that their proposed sensor involved POF achieved a remarkable sensitivity, which is 4284.8 nm/RIU, while proving the capability of POF sensors in multiple sensing applications such as RI and temperature sensing (L. Liu et al., 2021).

POF is said to be durable compared to silica glass, as many previous works claimed that fiber sensor probe with POF is robust and reliable. Zeni et al. mentioned that they managed to fabricate a reliable and robust POF-SPR sensor for therapeutic antibody detection in human serum (Zeni et al., 2020). However, it cannot withstand high temperature applications as the melting point of polymer is only 80°C. Despite this limitation, the application of POF in temperature sensors has also been studied. For example, research by L. Liu et al. proposed a POF sensor to detect RI and temperature changes as mentioned before (L. Liu et al., 2021). Moreover, POF has still been chosen for various applications that do not involve high temperatures. Due to their durability, robustness, and versatility, POF can be modified into various geometries like U-bent, tapered, polished, screwed-shaped, and many more. Xue et al. reported that their proposed screw-shaped fiber sensor obtained high sensitivity, which is up to 0.52 dB/mm, even though during liquid level measurement, the sensitivity decreases with time. Besides, the POF has also been twisted to achieve a screw shape, showing the flexibility and how convenient the POF is. This research proves that POF is a strong candidate to be used in fiber sensors and needs to be studied to improve performance (Xue et al., 2020). With all of these advantages and limitations, POF has been a good choice for optical sensors, and more studies need to be done to improve the limitations, such as modifying the geometry of POF and additional materials for POF sensors.

2.4.2 Geometry of POF SPR Based Sensor

The flexibility of POF led to versatility, where it can be modified into different geometries to improve the sensitivity and detection capabilities. The geometry of a fiber optic is a critical characteristic in optimizing the performance of the sensor, as it can affect the waveguide of light transmitted during the sensing performance. Over the past decade, few types of geometries have been introduced, including U-bent, D-shaped, tapered, side-polished, and double-polished configurations. D-shaped POF has been chosen as a good candidate for improving the performance of the sensor. For instance, Wu et al. demonstrated that D-shaped SPR POF sensor can be used in biomedical applications, as they mentioned that low-RI POF shows significant sensitivity enhancement. Their proposed sensor achieved LOD of 0.95 μg/ml with a fast response